2D Colloidal Crystals with Anisotropic Impurities

Ya Chen,[1] Xinlan Tan,[1] Huaguang Wang,[1,2,*] Zexin Zhang,[1,2,†] J. M. Kosterlitz,[3] and Xinsheng Sean Ling[3,‡]
[1]Institute for Advanced Study, Center for Soft Condensed Matter Physics and Interdisciplinary Research, School of Physical Science and Technology, Soochow University, Suzhou 215006, China
[2]College of Chemistry, Chemical Engineering and Materials Science, Soochow University, Suzhou 215123, China
[3]Department of Physics, Brown University, Providence, Rhode Island 02912, USA

(Received 3 March 2021; revised 13 April 2021; accepted 4 June 2021; published 2 July 2021)

We report a study of 2D colloidal crystals with anisotropic ellipsoid impurities using video microscopy. It is found that at low impurity densities, the impurity particles behave like floating disorder with which the quasi-long-range orientational order survives and the elasticity of the system is actually enhanced. There is a critical impurity density above which the 2D crystal loses the quasi-long-range orientational order. At high impurity densities, the 2D crystal breaks into polycrystalline domains separated by grain boundaries where the impurity particles aggregate. This transition is accompanied by a decrease in the elastic moduli, and it is associated with strong heterogeneous dynamics in the system. The correlation length vs impurity density in the disordered phase exhibits an essential singularity at the critical impurity density.

DOI: 10.1103/PhysRevLett.127.018004

Impurities are ubiquitous in crystals trapped during crystal growth [1]. They can significantly change the physical properties of the host crystals [2]. Understanding the effects of the impurities on the structures and dynamics of the crystal [3–5] has been an important task in condensed matter physics. It was pointed out by Larkin [4] and later by Imry and Ma [6] that impurities may have benign or devastating effects on the ordering of the host crystal lattice depending on how they interact with the lattice. Because of the separation of energy scales, e.g., the rigidity of the atomic lattice is several orders of magnitude larger than that of the vortex lattice formed inside a type-II superconductor, thus it was widely believed that an arbitrary amount of atomic "quenched disorder" will act like a random pinning potential landscape that will destroy the crystalline order in the soft vortex lattice. This so-called Larkin-Imry-Ma effect [4,6] was indeed observed experimentally in 2D colloidal crystals with a random pinning potential created by a disordered substrate [7]. For systems with no obvious separation of energy scales between those particles forming the lattice and those deemed to be impurities, the physical picture is not at all clear. It was conjectured [4] that at low concentration of atomic impurities, they should behave as "floating" defects, having minor effects on the order of the lattice. At high concentrations, however, the effect of these impurities on the order of the host lattice is not well understood. In fact, adding impurities to metals to enhance their mechanical strength is a well-known method in metallurgy [8] although the underlying physics is poorly understood.

In this Letter, we explore these issues by using a 2D colloidal model system. The colloidal particles can be directly observed using optical microscopy [9], making the colloidal system a convenient model for studying the phase behaviors of crystals with impurities [10]. A colloidal crystal is generally composed of monodispersed microspheres, and the common way of introducing impurities is adding spheres of a different size to the system [11–17]. For example, smaller spheres were added to a colloidal crystal as impurities, and the changes in structures and dynamics of the system were observed [16,17]. Recently, the shape anisotropy of particles has emerged as an important factor in the phase behavior [18–20] and dynamics [21]. One immediate question is, What are the effects of impurities with an anisotropic shape in the phase behavior and dynamics of a 2D colloidal crystal consisted of spheres?

In this experiment, we use ellipsoids as impurities in a 2D colloidal crystal and investigate the structure, elasticity, and dynamics of the resulting system. We find that structural defects form around the impurities and the orientational correlation exhibits a change from quasi-long-range to short-range order, i.e., an order-disorder transition, above a critical impurity density that can be characterized using the concepts from the Kosterlitz-Thouless-Halperin-Nelson-Young (KTHNY) theory. We find that with increasing impurity density, the elastic constant of the system shows an enhancement at first, similar to impurity enhancement in metals [8], and then exhibits a sharp decrease at high impurity densities associated with the appearance of heterogeneous dynamics. However, the dynamics of the system behaves monotonically with increasing impurity density. The findings shed new light into the correlations between microstructures, dynamics, and macroscopic properties in colloidal crystal with impurities.

In our experiments, the colloidal crystal was composed of polystyrene (PS) spheres (nominal diameters

$\sigma_s = 2.5$ μm, Duke Scientific). The impurities were ellipsoids (long axis $a = 13.4$ μm and short axis $b = 2.2$ μm), fabricated by a common stretching method [22]. To introduce the impurities, we mixed the spheres and ellipsoids in an aqueous solution of 3 mM sodium dodecyl sulfate (SDS) and confined a tiny drop of the mixture between two glass coverslips with a spacing of $\sim 1.1\sigma_s$ to form monolayer samples. The SDS is used to stabilize the particles in the aqueous solution. At the ionic strength in the aqueous solution (3 mM) the particles have a Debye length of $\sim$20 nm. Thus for the phase behavior, the colloidal particles can be considered as hard particles [18,21]. The areal fraction of the sample was calculated as $\phi_{\text{all}} = [n_s\pi(\sigma_s/2)^2 + n_e\pi ab/4)]/A_T$, where $n_s(n_e)$ is the number of sphere (ellipsoid) particles in the field of view, A_T is total area of the field of view. Our experiments employed the colloidal samples with a constant ϕ_{all}, $\sim$0.89, and varied impurity density, i.e., area fraction of impurity (ϕ). This enabled us to trace sample evolution as a function of impurity density. Video microscopy (Zeiss Observer A1) was used to collect image data with a CCD camera (Basler ACE) at a rate of 3 frames per second. Before each measurement, the sample was allowed to equilibrate for up to 8 h, and during the measurement the number of particles in the field of view remained constant and no drift was observed. The positions of the centers of individual particles were obtained using the open source program ImageJ(NIH). The spatial resolution was 60 nm.

Figure 1(a) shows the typical micrographs of the systems with different impurity concentrations. In the absence of ellipsoidal impurities, the colloidal spheres form ordered structures representing a 2D crystal phase. In the presence of a finite concentration of impurities, structural defects such as disclinations and edge dislocations form around these impurity particles. Such structural change can be clearly characterized by Voronoi diagrams [23] [Fig. 1(b)]. The color denotes the number of the nearest neighbors (n_i) for particle i, which can semiquantitatively characterize the structures in 2D [24]. $n_i = 6$ indicates the ordered structures while $n_i \neq 6$ denotes the disordered structures [24]. With increasing density of impurities, the number of particles with $n_i \neq 6$ increases as expected so that the defect density increases. It is observed that the defects are localized around the ellipsoids.

To further precisely capture the structural evolution induced by the ellipsoids, the ordering of each particle is quantified by calculating the bond orientational order parameter: $\psi_{6i} = 1/n_i \sum_{j=1}^{n_i} e^{i6\theta_{ij}}$, where the sum goes over all n_i nearest neighbors of particle i, θ_{ij} is the angle of the jth bond in respect to a reference axis. This parameter has been widely used to quantify the crystalline ordering in 2D systems composed of spheres [25–29]. Note that $|\psi_{6i}| = 1$ means the perfect hexagonal arrangement of six nearest-neighbor particles around the ith particle and $|\psi_{6i}| \sim 0$ means that the nearest-neighbor particles deviate

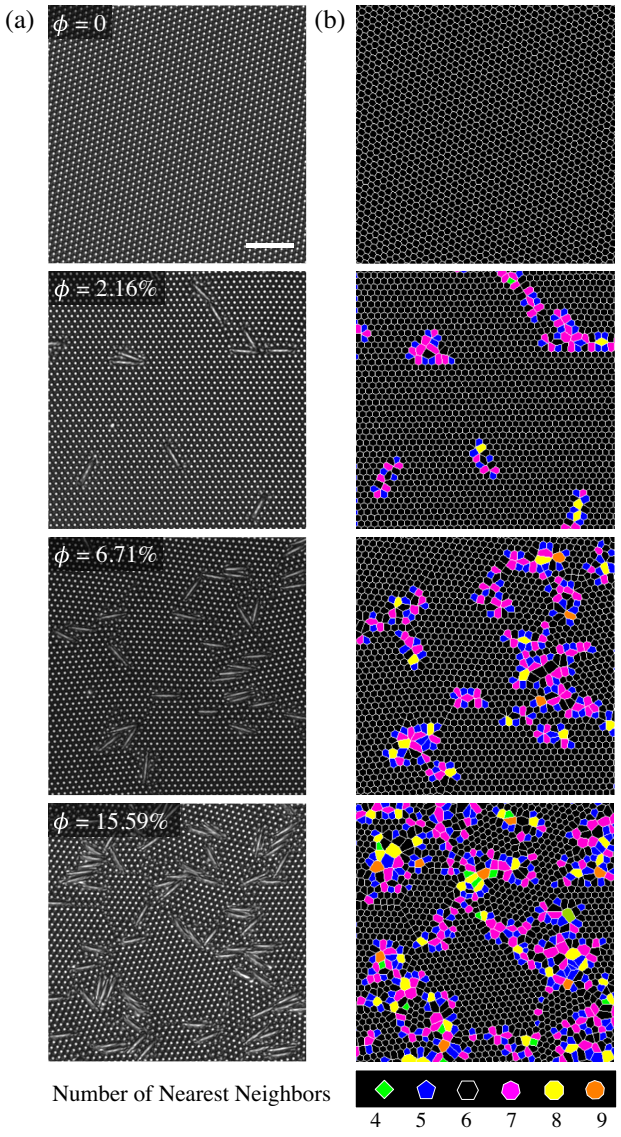

FIG. 1. (a) Brightfield micrographs of monolayers of spheres and ellipsoids at different ellipsoid densities (ϕ). (b) The corresponding Voronoi diagrams. The scale bar is 20 μm and applies to all graphs.

from the hexagonal arrangement indicating a disorder structure [25–29]. Figure 2(a) shows that $|\psi_{6i}|$ of the spheres around the ellipsoids tend to smaller values than that of the spheres away from the ellipsoids. This confirms that the defects originate from the ellipsoid impurities. As the impurity concentration increases, the ellipsoids tend to aggregate. We conjecture that there is an effective attraction between the ellipsoid particles mediated by the host lattice, similar to how interstitials and vacancies attract each other in a 2D crystal [30]. The impurity aggregates tend to break the host lattice into domains of ordered regions.

At very low densities, the impurities rarely form aggregates and they have minimal effects on the ordering of the 2D crystal, i.e., the quasi-long-range o rder survives.

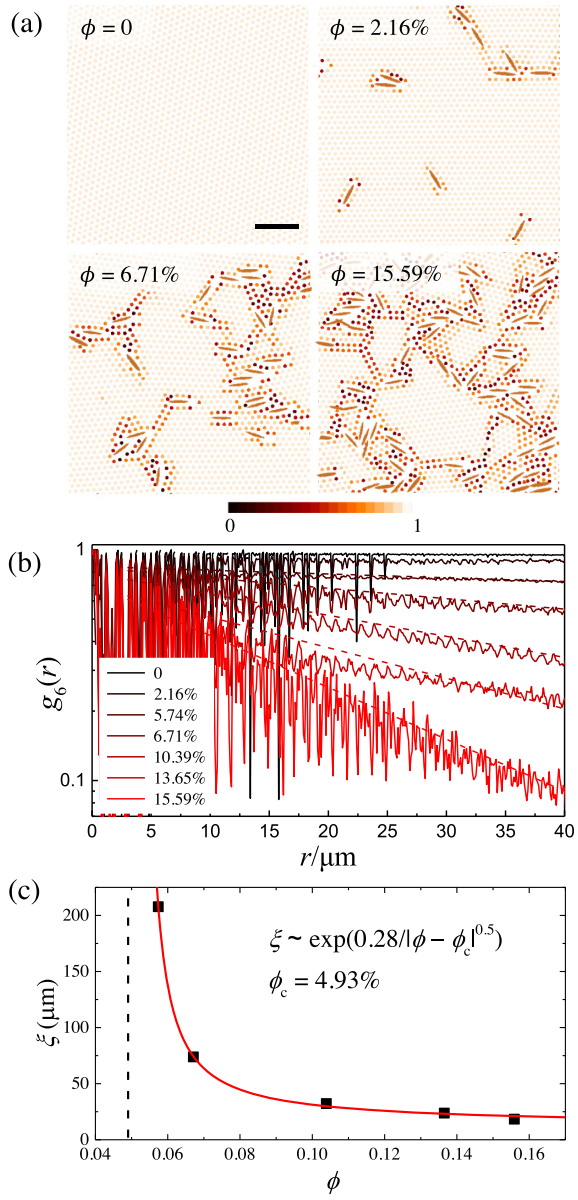

FIG. 2. (a) Spatial distributions of the bond orientational order parameter $|\psi_{6i}|$ at different ellipsoid densities (ϕ). The ellipsoids are marked by orange ellipses. The scale bar is 20 μm and applies to all graphs. (b) Orientational correlation function at different ϕ. The dashed curves are fits of $g_6(r)$ to $e^{-r/\xi}$. (c) ξ vs ϕ. The data suggest an essential singularity at $\phi_c = 0.049 \pm 0.001$, as indicated by the fitting curve (in red). The dashed line marks the critical impurity density.

In contrast, at high impurity densities the defective regions seem to percolate through the whole system and there exist only local crystalline domains. As a result the system becomes highly heterogeneous. We suggest that at high densities, the impurities spontaneously aggregate to form effective pinning centers, i.e., becoming a type of quenched disorder, resulting in the breakdown of the quasi-long-range order. To clarify this observation, the orientational correlation function is calculated; $g_6(r = |r_i - r_j|) = \langle \psi_{6i}^*(r_i)\psi_{6j}(r_j)\rangle$, where r_i and r_j are the positions of particles i and j [24]. Figure 2(b) shows the results of $g_6(r)$ at different impurity densities. At $\phi = 0$, $g_6(r)$ is constant with r, which demonstrates the orientational long-range order of the 2D crystal. At $\phi = 0.0216$, $g_6(r)$ is compatible with algebraic decay, suggesting quasi-long-range orientational order of a hexatic phase, confirming that at low impurity density the impurity particles behave as floating disorder [4]. At high impurity densities ($\phi > 0.0216$), $g_6(r)$ shows exponential decay, associated with short-range orientational order, verifying that the impurity induced quenched disorder drives the system disordered. This is consistent with the KTHNY theory, demonstrating a two-step order-disorder transition with increasing impurities that is similar to the 2D melting of paramagnetic colloidal crystals [31]. The data suggest that there is a critical impurity density above which the 2D crystal loses the quasi long-range orientational order. This is consistent with some aspects of the early theoretical studies of 2D XY models with disorder [32,33] and the experimental work of colloidal crystal with sphere impurities [17]. It should be noted that our anisotropic impurity induced order-disorder transition differs significantly from the 2D melting with anisotropic interparticle interactions where the KTHNY scenario of isotropic melting is modified and a smecticlike phase is observed [34].

To quantify the impurity-induced order-disorder transition, the characteristic length (ξ) of the orientational correlation is obtained by fitting the $g_6(r)$ data to an exponential decay form $e^{-r/\xi}$. It is interesting to find that ξ exhibits an essential singularity $\xi \sim \exp(b/|\phi - \phi_c|^{0.5})$ with $\phi_c = 0.0493$ [Fig. 2(c)], which demonstrates the existence of a critical impurity density. This essential singularity was the hallmark of the KTHNY theory [35–37] that has been confirmed in many experimental studies of 2D melting [24,26,38].

Next, we focus on the dynamics of the system influenced by the ellipsoid impurities. Here, to avoid the long-wavelength elastic deformations in the 2D system, the relative position $\mathbf{r}' = \mathbf{r} - \langle \mathbf{r}_k \rangle$ is used for characterizing the dynamics, where $\mathbf{r}_k$ is the position of the near neighbor and the bracket denotes the average over all near neighbors [39,40]. We first calculated the mean square displacements at different impurity densities: $\langle \Delta r^2(t) \rangle = \langle |\mathbf{r}'(t) - \mathbf{r}'(0)|^2 \rangle$. As impurity density increases, $\langle \Delta r^2 \rangle$ increases [Fig. 3(a)] demonstrating a faster dynamics with more impurities. However, $\langle \Delta r^2 \rangle$ shows a plateau independent of the impurity density in the experimental time windows. This demonstrates that the system exhibits confined dynamics, namely, the particles appear to be caged in by their neighbors. To elucidate the origin of the fast dynamics, the $\langle \Delta r^2 \rangle$ of ordered particles and disordered particles were calculated [Fig. 3(b)]. Here the ordered (disordered) particles are defined as the particles with $\psi_6 \geq 0.8 (\psi_6 < 0.8)$. The result shows that the $\langle \Delta r^2 \rangle$ of

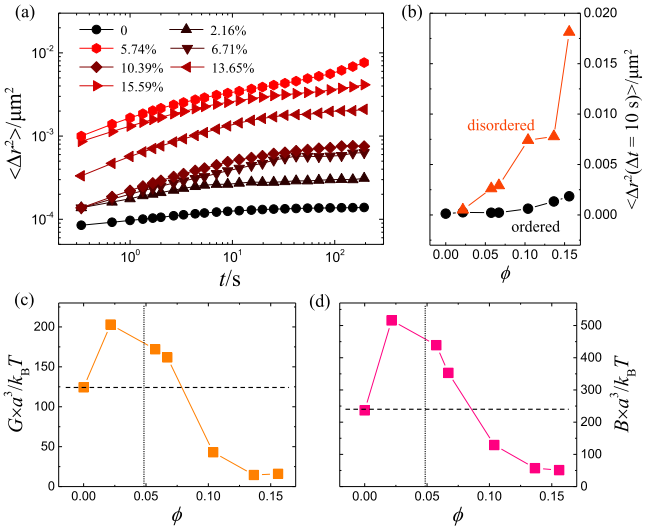

FIG. 3. (a) Mean square displacements at different ellipsoid densities (ϕ). (b) Mean square displacements of ordered particles and disordered particles for lag time = 10 s. Different choice of the lag time yields similar results. (c) Shear modulus at different ϕ. (d) Bulk modulus at different ϕ. The moduli are given in units of k_BT/a^3, with a the lattice constant. The vertical dotted lines mark the critical impurity density, and the horizontal dashed lines label the moduli for the crystal without impurities.

ordered particles is almost the same independent of the impurity density, while the $\langle \Delta r^2 \rangle$ of disordered particles increases with increasing the impurity density which dominates the enhancement of the dynamics of the systems. Such enhanced dynamics originates from the destruction of the periodic crystalline structure due to the disorder, which lowers the energy barrier for thermally activated motion [41,42].

We find that with increasing impurity density, there is a nonmonotonic change of mechanical properties. However, the dynamics of the system experiences a monotonic increase due to the increased disordering. This is clarified by analyzing the elastic moduli of the system. The elastic moduli of a 2D colloidal crystal can be measured from the dispersion relations calculated from displacement covariance matrices (see Supplemental Material [43]) [44–47]. The obtained shear and bulk moduli for the system without impurities [Fig. 3(c)] are consistent with those of 2D colloidal crystal measured in the previous work [48]. When the impurity density rises, increases of the elastic moduli are found. This effect is similar to impurity strengthening in metallurgy [8]. Once the impurity density further increases beyond ϕ_c, the elastic moduli experience a monotonic decrease and at last reach small values lower than those of the crystal without impurities. One might be surprised that there is no sharp drop in shear modulus at ϕ_c. Strictly speaking, the shear modulus dropping to zero at the KTHNY melting transition is only for infinite time and length scales. For measurements at finite time and length scales such as this experiment, no sharp drop in the shear modulus G is expected at T_m, or ϕ_c here. Indeed, we find that the sharp drop in G occurs deep into the disordered phase, as expected from the dynamics of 2D melting [49].

The fast dynamics direct linking to the disordered structures in Fig. 3(b) is clearly reflected by the spatial distributions of particle displacements shown in Fig. 4(a). The fast-moving particles localized around the ellipsoids are associated with the disordered structures while the slow-moving particles correspond to the ordered structures [Fig. 1 and Fig. 2(a)]. These thereby lead to dynamical heterogeneity at high impurity densities, demonstrating a direct link between structures and heterogeneous dynamics. The spatial distributions of displacements clearly indicate heterogeneous dynamics at high impurity densities. The heterogeneous dynamics is further characterized by calculating the four-point susceptibilities at different impurity densities [17,50] [Fig. 4(b)]: $\chi_4(a, \Delta t) = N[\langle Q_2(a, \Delta t)^2 \rangle - \langle Q_2(a, \Delta t) \rangle^2]$, where $Q_2(a, \Delta t) = 1/N \sum_{i=1}^{N} \exp(-\Delta r_i^2/2a^2)$ is the two-time self-correlation function, a is a preselected length scale to be probed, Δr_i^2 is the mean squared displacement of particle i in time Δt, and N is the total number of particles. Here $a = 0.5$ μm, and the other choices give a similar result. χ_4 is small at low impurity densities, corresponding to the homogeneous dynamics. This agrees with the observation that there are no obvious cooperative motions of the particles in the systems [Fig. 4(a)]. In contrast, at high impurity densities, χ_4 exhibits large value at long times corresponding to the heterogeneous dynamics. This is consistent with the significant cooperative motions reflected by the existence of the clusters of the fast-moving particles [Fig. 4(a)] originating from the increased disordered structures.

It is important to point out that at $\phi = 0.0216$, the statics of the system appears to be in the hexatic phase with quasi-long-range orientational order. The system shows homogeneous dynamics, which is different from the obvious heterogeneous dynamics in the hexatic phase of the 2D melting [51]. This distinction between the impurity induced disorder-order transition here and the normal 2D melting [51] is worthy of further study. Furthermore, the ellipsoid impurity induced dynamical heterogeneity at high impurity densities is in agreement with that found in 2D crystal with sphere impurities [17]. However, unlike the discontinuous jump of dynamical heterogeneity for the 2D crystal with sphere impurities [17], a gradual increase of the dynamical heterogeneity is found in the system with increasing ellipsoid impurities here. Moreover, besides the correlation between structures and heterogeneous dynamics, a relationship between the heterogeneous dynamics and the elasticity is revealed. At low impurity densities, there is an enhancement of the elastic moduli and the system exhibits homogeneous dynamics. At high impurity densities, the effective elastic

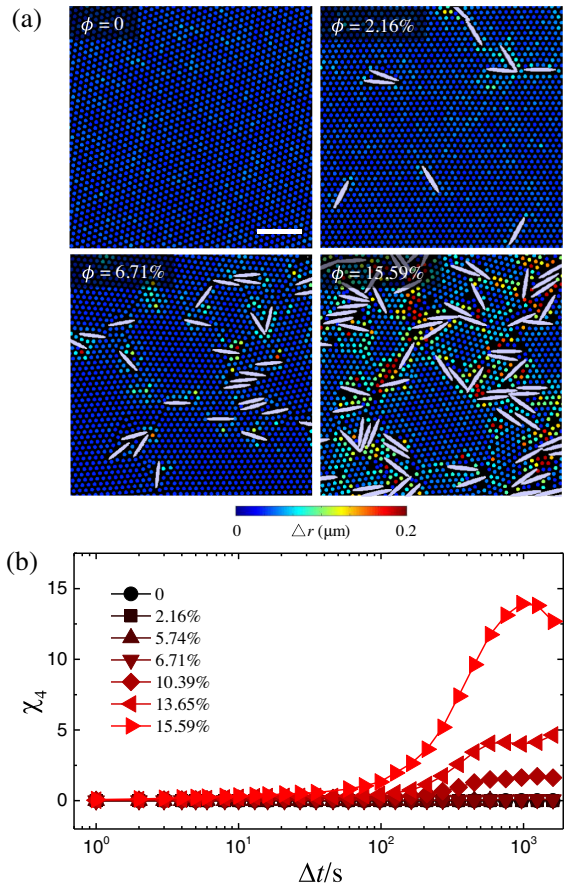

FIG. 4. Spatial distributions of displacements for lag time 200 s at different ellipsoid densities (ϕ). (b) Four-point susceptibility χ_4 at different ϕ. The scale bar is 20 μm and applies to all graphs.

moduli are lower than those of the host crystal and the heterogeneous dynamics is enhanced in the system.

In summary, we performed real-time video microscopy experiments on 2D colloidal crystals with ellipsoid impurities to study their effects on the structure, elasticity, and dynamics of the colloidal crystals. The results show that the impurities give rise to two kinds of disordering effects. At low densities, ellipsoid particles act as floating disorder as envisioned by Larkin [4], the quasi-long-range orientational order of the host lattice persists. At high densities, the impurity particles spontaneously aggregate at grain boundaries in the host lattice, destroying the quasi-long-range orientational order. The correlation length in the disordered phase as a function of the impurity density follows an essential singularity, similar to that in the KTHNY theory of 2D melting.

This work was financially supported by the National Natural Science Foundation of China (12074275 and 11704269), the Natural Science Foundation of the Jiangsu Higher Education Institutions of China (20KJA150008, 17KJB140020), and the PAPD program of Jiangsu Higher Education Institutions. J. M. K. acknowledges partial support from the Brown Theoretical Physics Center (BTPC).

*hgwang@suda.edu.cn
†zhangzx@suda.edu.cn
‡xinsheng_ling@brown.edu

[1] J. D. Weeks and G. H. Gilmer, Dynamics of crystal growth, Adv. Chem. Phys. **40**, 157 (1979).
[2] K. H. Höck and H. Thomas, Statics and dynamics of "soft" impurities in a crystal, Z. Med. Phys. B **27**, 267 (1977).
[3] A. Maradudin, Some effects of point defects on the vibrations of crystal lattices, Rep. Prog. Phys. **28**, 331 (1965).
[4] A. I. Larkin, Effect of inhomogeneities on the structure of the mixed state of superconductors, Zh. Éksp. Teor. Fiz. **58**, 1466 (1970) [Sov. Phys. JETP **31**, 784 (1970)].
[5] S. Martin, G. Bryant, and W. van Megen, Crystallization kinetics of polydisperse colloidal hard spheres: Experimental evidence for local fractionation, Phys. Rev. E **67**, 061405 (2003).
[6] Y. Imry and S.-K. Ma, Random-Field Instability of the Ordered State of Continuous Symmetry, Phys. Rev. Lett. **35**, 1399 (1975).
[7] A. Pertsinidis and X. S. Ling, Statics and Dynamics of 2d Colloidal Crystals in a Random Pinning Potential, Phys. Rev. Lett. **100**, 028303 (2008).
[8] A. H. Cottrell and B. A. Bilby, Dislocation theory of yielding and strain ageing of iron, Proc. Phys. Soc. A **62**, 49 (1949).
[9] H. Wang and Z. Zhang, Application of video microscopy in experimental soft matter physics, Acta Phys. Sin. **65**, 178705 (2016).
[10] B. Li, D. Zhou, and Y. Han, Assembly and phase transitions of colloidal crystals, Nat. Rev. Mater. **1**, 15011 (2016).
[11] S. R. Williams, I. K. Snook, and W. van Megen, Molecular dynamics study of the stability of the hard sphere glass, Phys. Rev. E **64**, 021506 (2001).
[12] P. Bartlett and P. B. Warren, Reentrant Melting in Polydispersed Hard Spheres, Phys. Rev. Lett. **82**, 1979 (1999).
[13] M. Fasolo and P. Sollich, Equilibrium Phase Behavior of Polydisperse Hard Spheres, Phys. Rev. Lett. **91**, 068301 (2003).
[14] S. Toxvaerd, U. R. Pedersen, T. B. Schrder, and J. C. Dyre, Stability of supercooled binary liquid mixtures, J. Chem. Phys. **130**, 224501 (2009).
[15] Z. Zhang, N. Xu, D. T. N. Chen, P. Yunker, A. M. Alsayed, K. B. Aptowicz, P. Habdas, A. J. Liu, S. R. Nagel, and A. G. Yodh, Thermal vestige of the zero-temperature jamming transition, Nature (London) **459**, 230 (2009).
[16] P. Yunker, Z. Zhang, K. B. Aptowicz, and A. G. Yodh, Irreversible Rearrangements, Correlated Domains, and Local Structure in Aging Glasses, Phys. Rev. Lett. **103**, 115701 (2009).
[17] P. Yunker, Z. Zhang, and A. G. Yodh, Observation of the Disorder-Induced Crystal-to-Glass Transition, Phys. Rev. Lett. **104**, 015701 (2010).

[18] Z. Zheng, F. Wang, and Y. Han, Glass Transitions in Quasi-Two-Dimensional Suspensions of Colloidal Ellipsoids, Phys. Rev. Lett. **107**, 065702 (2011).
[19] K. Takae and A. Onuki, Formation of double glass in binary mixtures of anisotropic particles: Dynamic heterogeneities in rotations and displacements, Phys. Rev. E **88**, 042317 (2013).
[20] W. S. Xu, X. Duan, Z. Y. Sun, and L. J. An, Glass formation in a mixture of hard disks and hard ellipses, J. Chem. Phys. **142**, 224506 (2015).
[21] X. Liu, H. Wang, Z. Zhang, J. M. Kosterlitz, and X. S. Ling, Nature of the glass transition in 2d colloidal suspensions of short rods, New J. Phys. **22**, 103066 (2020).
[22] J. A. Champion, Y. K. Katare, and S. Mitragotri, Making polymeric micro-and nanoparticles of complex shapes, Proc. Natl. Acad. Sci. U.S.A. **104**, 11901 (2007).
[23] U. Gasser, Crystallization in three-and two-dimensional colloidal suspensions, J. Phys. Condens. Matter **21**, 203101 (2009).
[24] Y. Han, N. Y. Ha, A. M. Alsayed, and A. G. Yodh, Melting of two-dimensional tunable-diameter colloidal crystals, Phys. Rev. E **77**, 041406 (2008).
[25] K. Watanabe and H. Tanaka, Direct Observation of Medium-Range Crystalline Order in Granular Liquids Near the Glass Transition, Phys. Rev. Lett. **100**, 158002 (2008).
[26] S. Deutschlander, T. Horn, H. Lowen, G. Maret, and P. Keim, Two-Dimensional Melting Under Quenched Disorder, Phys. Rev. Lett. **111**, 098301 (2013).
[27] E. P. Bernard and W. Krauth, Two-Step Melting In Two Dimensions: First-Order Liquid-Hexatic Transition, Phys. Rev. Lett. **107**, 155704 (2011).
[28] R. Zangi and S. A. Rice, Freezing transition and correlated motion in a quasi-two-dimensional colloid suspension, Phys. Rev. E **68**, 061508 (2003).
[29] T. Kawasaki, T. Araki, and H. Tanaka, Correlation Between Dynamic Heterogeneity and Medium-Range Order in Two-Dimensional Glass-Forming Liquids, Phys. Rev. Lett. **99**, 215701 (2007).
[30] W. Lechner, D. Polster, G. Maret, P. Keim, and C. Dellago, Self-organized defect strings in two-dimensional crystals, Phys. Rev. E **88**, 060402(R) (2013).
[31] K. Zahn, R. Lenke, and G. Maret, Two-Stage Melting of Paramagnetic Colloidal Crystals in Two Dimensions, Phys. Rev. Lett. **82**, 2721 (1999).
[32] M. Rubinstein, B. Shraiman, and D. R. Nelson, Two-dimensional XY magnets with random Dzyaloshinskii-Moriya interactions, Phys. Rev. B **27**, 1800 (1983).
[33] D. Carpentier and P. L. Doussal, Topological transitions and freezing in XY models and coulomb gases with quenched disorder: Renormalization via traveling waves, Nucl. Phys. **B588**, 565 (1999).
[34] C. Eisenmann, U. Gasser, P. Keim, and G. Maret, Anisotropic Defect-Mediated Melting of Two-Dimensional Colloidal Crystals, Phys. Rev. Lett. **93**, 105702 (2004).
[35] J. M. Kosterlitz and D. J. Thouless, Ordering, metastability and phase-transitions in 2 dimensional systems, J. Phys. C **6**, 1181 (1973).
[36] B. I. Halperin and D. R. Nelson, Theory of 2-Dimensional Melting, Phys. Rev. Lett. **41**, 121 (1978).
[37] A. P. Young, Melting and the vector coulomb gas in 2 dimensions, Phys. Rev. B **19**, 1855 (1979).
[38] P. Keim, G. Maret, and H. H. von Grnberg, Franks constant in the hexatic phase, Phys. Rev. E **75**, 031402 (2007).
[39] S. Vivek, C. P. Kelleher, P. M. Chaikin, and E. R. Weeks, Long-wavelength fluctuations and the glass transition in two dimensions and three dimensions, Proc. Natl. Acad. Sci. U.S.A. **114**, 1850 (2017).
[40] B. Illing, S. Fritschi, H. Kaiser, C. L. Klix, G. Maret, and P. Keim, Merminwagner fluctuations in 2d amorphous solids, Proc. Natl. Acad. Sci. U.S.A. **114**, 1856 (2017).
[41] F. Nabarro, *Theory of Crystal Dislocations* (Dover Publications, New York, 1987), Vol. 264, ISBN-10: 0486654885.
[42] A. Pertsinidis and X. S. Ling, Equilibrium Configurations and Energetics of Point Defects in Two-Dimensional Colloidal Crystals, Phys. Rev. Lett. **87**, 098303 (2001).
[43] See Supplemental Material at http://link.aps.org/supplemental/10.1103/PhysRevLett.127.018004 for data on elastic moduli.
[44] T. Still, C. P. Goodrich, K. Chen, P. J. Yunker, S. Schoenholz, A. J. Liu, and A. G. Yodh, Phonon dispersion and elastic moduli of two-dimensional disordered colloidal packings of soft particles with frictional interactions, Phys. Rev. E **89**, 012301 (2014).
[45] H. H. von Grünberg, P. Keim, K. Zahn, and G. Maret, Elastic Behavior of a Two-Dimensional Crystal Near Melting, Phys. Rev. Lett. **93**, 255703 (2004).
[46] K. Chen, W. G. Ellenbroek, Z. X. Zhang, D. T. N. Chen, P. J. Yunker, S. Henkes, C. Brito, O. Dauchot, W. van Saarloos, A. J. Liu, and A. G. Yodh, Low-Frequency Vibrations of Soft Colloidal Glasses, Phys. Rev. Lett. **105**, 025501 (2010).
[47] P. Keim, G. Maret, U. Herz, and H. H. von Grünberg, Harmonic Lattice Behavior of Two-Dimensional Colloidal Crystals, Phys. Rev. Lett. **92**, 215504 (2004).
[48] B. Li, F. Wang, D. Zhou, Y. Peng, R. Ni, and Y. Han, Modes of surface premelting in colloidal crystals composed of attractive particles, Nature (London) **531**, 485 (2016).
[49] A. Zippelius, B. I. Halperin, and D. R. Nelson, Dynamics of two-dimensional melting, Phys. Rev. B **22**, 2514 (1980).
[50] L. Berthier, G. Biroli, J. P. Bouchaud, L. Cipelletti1, D. El Masri, D. L'Hote, F. Ladieu, and M. Pierno, Direct experimental evidence of a growing length scale accompanying the glass transition, Science **310**, 1797 (2005).
[51] K. Zahn and G. Maret, Dynamic Criteria for Melting in Two Dimensions, Phys. Rev. Lett. **85**, 3656 (2000).